АКАДЕМИЯ НАУК УКРАИНСКОЙ ССР
ИНСТИТУТ ТЕОРЕТИЧЕСКОЙ ФИЗИКИ
ISSN 0206-3824

ФИЗИКА МНОГОЧАСТИЧНЫХ СИСТЕМ

ФИЗИКА МНОГОЧАСТИЧНЫХ СИСТЕМ

АКАДЕМИЯ НАУК
УКРАИНСКОЙ ССР
ИНСТИТУТ ТЕОРЕТИЧЕСКОЙ ФИЗИКИ

МЕЖВЕДОМСТВЕННЫЙ
НАУЧНО-ТЕХНИЧЕСКИЙ
СБОРНИК
НАУЧНЫЕ ТРУДЫ

ОСНОВАН В 1982 г.

ВЫПУСК 19

КИЕВ НАУКОВА ДУМКА 1991

19
1991

Physics of Many-Particle Systems, Vol. 19, pp 37-50 (1991)
E.S. Kryachko, ed., Naukova Dumka, Kiev

M. M e z e i

THE THEORY OF HYDROGEN BONDING IN WATER

1. Introduction

The water molecule itself is small and deceptively simple. However, its condensed phases have several remarkable properties. In the solid phase, it can take an unusually high number of crystalline forms and it is also capable to form an amorphous (glassy) solid. Upon melting, contrary to conventional wisdom, it contracts which is rather rare. Furthermore, its volume continues to decrease as the temperature is increased, leading to a density maximum at 4°C — a phenomenon almost unique to water. Other, equally puzzling anomalies include the large specific heat and the large isothermal compressibility of liquid water. Lang and Ludemann reviewed recently the water anomalies [44].

The source of this anomalous behaviour of water can be traced to the peculiar way that water molecules interact with each other, i.e. to the particular characteristics of the water- water hydrogen bond. The purpose of this paper is to describe the water-water hydrogen bond and its role in the various physical properties of liquid water.

2. Relation between the properties of a liquid and the intermolecular interactions

According to the basic tenets of statistical mechanics, the properties of a liquid are uniquely determined from the potential energy function as the Boltzmann-weighted average over all configurations. For a system of N particles, the Boltzmann average of a property Q in the canonical ensembleis given as

$$\langle Q\rangle = \int Q(\mathbf{X}^N)\exp[-E(\mathbf{X}^N)/kT]d\mathbf{X}^N/\exp[-E(\mathbf{X}^N)/kT]d\mathbf{X}^N \qquad (1)$$

where k is the Boltzmann constant, T is the absolute temperature and $E(\mathbf{X}^N)$ and $Q(\mathbf{X}^N)$ are the total energy and the property Q at the N-particle configuration $\mathbf{X}^N$, respectively. Eq. (1) can be considered a weighted average of Q, and thus $\exp[-E(\mathbf{X}^N)/kT]$ is referred to as the Boltzmann weight (the numerator of Eq. (1) serves to normalize it). Equations similar in form to (1) hold in other statistical ensembles. As N tends to infinity, the limit of Q becomes independent of the choice of the statistical ensemble and will give the liquid value. For liquid water (far from the critical point), a collection of O(100) particles under periodic boundary conditions appears to approach this limit sufficiently.

The evaluation of the integrals in (1) is a formidable task in general since the configurational space involved is $6(N\text{-}1)$ dimensional. Restricting the form of the function $E(\mathbf{X}^N)$ to certain manageable types, approximative solutions can be found, either by computer simulation or by integral equation techniques. Computer simulation generates a finite sample

of Boltzmann-weighted configurations allowing the calculation of the properties of interest as simple averages over these configurations. The techniques used to generate these configurations may be probabilistic or deterministic. Probabilistic methods, called Monte Carlo methods, introduced by Metropolis et al. [48] use an importance sampling technique while the deterministic route, called molecular dynamics, follows Newton's law (or its generalization in other ensembles) to generate physically meaningful trajectories — the ergodic theorem ensures that these configurations too will follow the Boltzmann distribution. Integral equations, on the other hand, are obtained by imposing a so called closure relationship on a hierarchy of distribution functions. The solutions to these equations, substituted into Eq. (1) can yield the liquid properties. The success of these descriptions, besides overcoming the numerical difficulties posed by slowly convergent or divergent iterations, hinges upon the choice of the closure relation. The RISM method has been extended to molecules with charged sites by Hirata and Rossky [34] and applied to liquid water by Pettitt and Rossky [62]. However, as the error introduced by the closure relation assumed can only be assessed empirically, most studies on liquid water used computer simulation.

From the discussion above it is clear that the property of a liquid is in principle a function of the energy of the complete configurations. To elucidate the role of interactions between neighbouring molecules, i.e. in case of water, the role of the hydrogen bond, it is necessary to study the dependence of $E(\mathbf{X}^N)$ on the contributions from the individual hydrogen bonds in the configuration $\mathbf{X}^N$.

3. Water clusters

3.1. The linear dimer

Our understanding of the hydrogen bond in water is based on the description of the water dimer. Physico-chemical intuition, based on the polarity of the O-H bond, suggests an O...H-O type arrangement, with the hydrogens not participating in the hydrogen bond forming a trans arrangement to reduce the repulsion. This view is supported by the tetrahedral arrangement of the water molecules in Ice Ih observed by X-ray diffraction. Theoretical calculations at successively higher level of approximations confirmed that intuition, proving that the (trans) linear hydrogen bond between two waters at $\sim$3.0 Å O-O distance leads to a minimum in the dimer energy surface at about 5-6 kcal/mol. Calculations by Finney, Quinn and Baum [2,25] showed that changing the non-bonding hydrogen of the donor water into the cis conformation raises the energy only by about 1 kcal/mol. Figure 1 shows a linear dimer, minimized at the MP2/6-31G* level [31,32] (SCF with the 6-31G* level plus second order Moller-Plessett perturbation correction) by Dannenberg [20] with a calculated dimerization energy of -6.40 kcal/mol. Evaluation of microwave spectra is essentially in agreement with the calculations, although the model used to evaluate the data assumed the general features of a linear hydrogen bond. The closeness of the H-O-H angle (105°) to the tetrahedral angle (109°) and the "acceptor angle" to the half of the tetrahedral angle makes the linear hydrogen bond a suitable building block of large hydrogen-bonded networks since the two acceptor directions and the two O-H bonds define four nearly equivalent directions. This can give rise to a variety of extended chains of hydrogen bonds where each water can form four hydrogen bonds. As waters are not forced to keep potential hydrogen-bonding sites unused due to the impossibility of finding partners, the network will be unusually strong. The near

equivalence of the four hydrogen-bonding directions allows an orientational variability that will reduce the entropic penalty of forming strongly bonded networks.

3.2. Bifurcated and trifurcated water dimers

While there are excellent methods to find a local minimum on a surface, the determination of the global minimum has long frustrated mathematicians and scientists alike. As the water dimer energy surface is six-dimensional, there is reason to suspect that the linear dimers are not the only minima or, due to the complexity of the competing interactions there might be regions far from the linear dimers that have comparable energy. In chemical terms, it can be argued that while the water dimer forming a single linear hydrogen bond is clearly optimizing the strength of that single bond, it might be possible to find other arrangements that allow more than one, albeit individually imperfect, hydrogen bonds to form with a net result that is comparable to the strength of the single linear hydrogen bond.

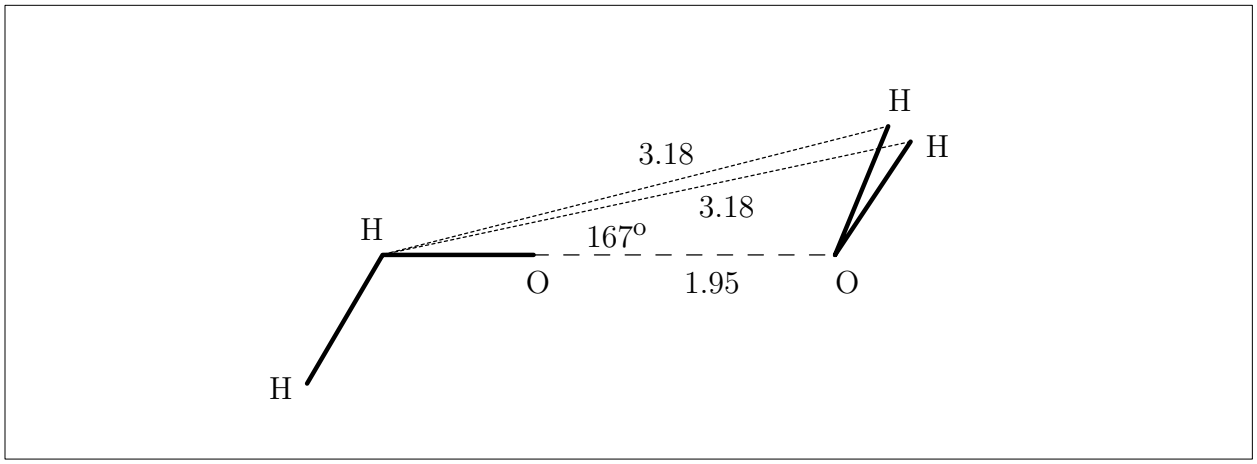

Fig. 1. Minimum-energy water dimer with linear hydrogen bond. Distances are in Å. Hydrogen bond is shown with broken line.

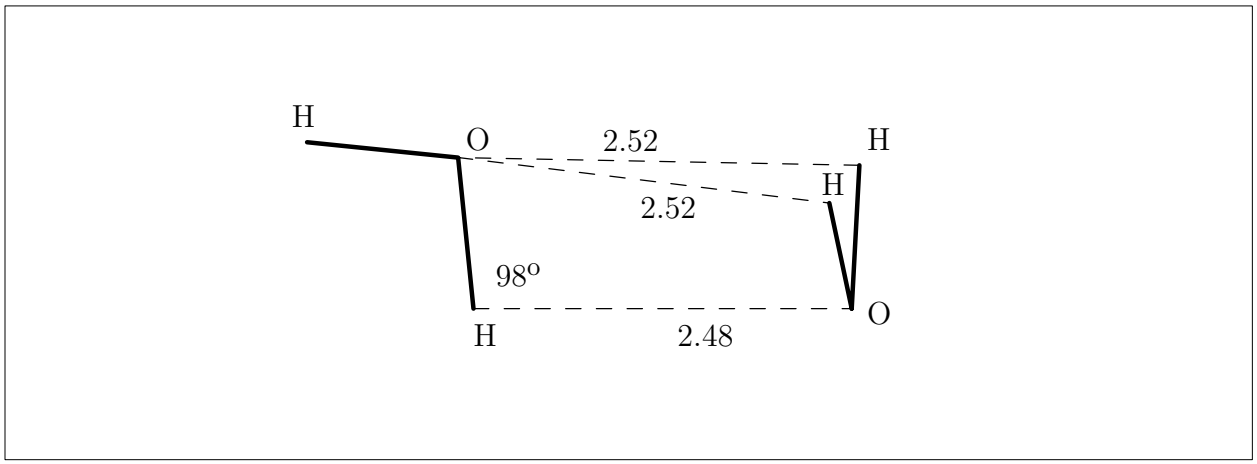

Fig. 2. Low-energy water dimer with trifurcated hydrogen bond. Distances are in Å. Hydrogen bonds are shown with broken line.

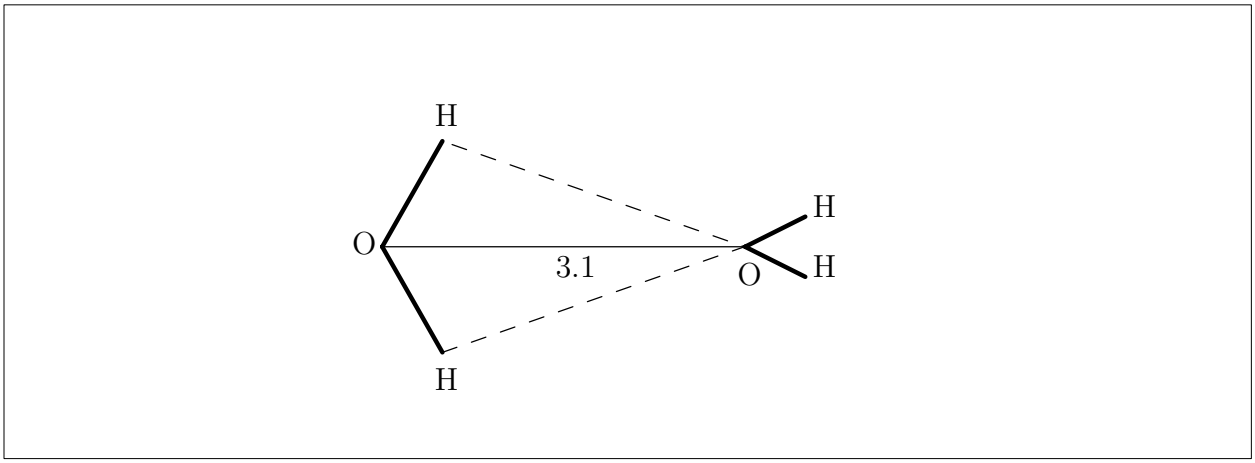

Fig. 3. Low-energy water dimer with bifurcated hydrogen bond. Distance is in Å. Hydrogen bonds are shown with broken line.

Finney and Baum exended their studies of the dimer surface using large-basis set ab initio calculations to consider a bifurcated structure [2], shown on Figure 2. With the two molecular planes kept perpendicular and the dipoles parallel, a shallow energy minimum was observed at cca 3.1 Å O-O distance that is about 2.5 kcal/mol weaker than the linear hydrogen bond.

Prompted by a study of the water dimer with the semiempirical AM1 method [22], Dannenberg recently performed a series of ab initio calculations that showed that a trifurcated structure, shown of Figure 3, has nearly as low energy as the linear dimer, -6.02 kcal/mol at the MP2/6-31G* level [20] (reminding us once again that attention to the global minimum problem can not be replaced by intuition). Its role in the liquid is likely to be less important than the linear dimer's since it can not be used in the formation of extended networks. It may be significant, however, in situations where a few water molecules are found isolated.

3.3. Water oligomers

In the consideration of molecular clusters one of the foremost questions is the possibility of describing the cluster based on information on the dimer alone, i.e. the degree to which the given intermolecular interactions can be considered to be pairwise additive. For water the first quantitative answer was obtained by Hankins, Stillinger and Moskowitz, who considered water trimers in various hydrogen-bonding orientations [30]. The trimer energy consistently differed from the sum of the dimer energies by 10-15% in the vicinity of the equilibrium dimer O-O distance, but its sign depended on the conformation. Similar conclusions were drawn later by Clementi et al. [19].

3.4. The role of electrostatics in water-water interactions

In the discussion above the formation of the water dimer was dominated by the electrostatic interaction, even though it is clear that, particularly at closer distances, classical

physics can not describe adequately the hydrogen bond. Electrostatics takes over, however, rather soon: the difference between the quantum-mechanically calculated dimer energies (at the Hartree- Fock level [63]) and the corresponding classical electrostatic interaction based on the quantum-mechanically calculated monomer charge density (with induced dipole interactions included) amount to only a few percent of the interaction energy for O-O distances of 5 Å or larger [53].

While the interaction between waters at hydrogen-bonding or closer distances have significant non-electrostatic component, Clementi et al. [19], based on the study of 28 water trimers, found that the nonadditive contribution to the energy can largely be explained by the polarization of the water electron density due to the electric field of its neighbours.

4. Modeling water-water interactions

While the importance of cooperative contributions was always recognized, computational restrictions necessitated the use of pairwise additive potentials, i.e. potentials that contain terms for each pair of molecules that are independent of the position of the rest of the system. To minimize the effect of neglecting the cooperative contributions, the potentials were parametrized to include these contribution in an average fashion. For this reason they usually called effective pairwise additive potential. While there has been considerable success in modeling liquid water with effective pairwise additive potentials, it is important to note that their validity is restricted to the state they have been parametrized to — e.g. they will not describe well interfaces or a simple dimer. In most cases additional simplification was obtained by assuming that the intramolecular geometry of a water molecule can be kept fixed and by neglecting quantum effects.

4.1. Pairwise additive models

Pairwise additive models assume localized centers of interaction on the water molecule, where neither the position of these centers within the local water frame, nor the strength of the interaction is affected by the molecule's environment. The type of interactions considered for water water interactions include electrostatic (point charge, dipole or quadrupole, etc.), exchange repulsion (inverse twelfth power or exponential) and dispersion (inverse sixth power). The combination of this latter two is also called the Lennard-Jones potential.

Bernal and Fowler [9] proposed a model that turned out to be the prototype of several successful models: positive charges at the hydrogen sites and a negative charge at a site on the HOH bisector, offset from the oxygen by 0.15 Å, and a Lennard-Jones center on the oxygen.

Ben Naim and Stillinger proposed a model consisting of four tetrahedrally arranged charges (two of them positive and the other two negative and a Lennard-Jones center at the oxygen site [5]. A switching function was used to simultaneously turn off the electrostatic interactions and turn on the Lennard-Jones term. The potential parameters were designed to reproduce experimental data. It was the first water model to be tested by computer simulation by Rahman and Stillinger [65] — this work provided the basis of a refined version called the ST2 model [78].

Sarkisov, Dashevsky and Malenkov [70] developed a water model using Kitaigordsky potential functions ($1/r^6$+ exp type) [42] for non-bonded interactions and a double-exponential hydrogen-bonding potential, added to the "standard" electrostatic terms and calculated its thermodynamic and structural parameters with Monte-Carlo simulations. The parameters were determined by fitting to experimental data, notably the dimer vibrational spectrum.

Using a different approach, Clementi and coworkers obtained several water models by fitting the potential parameters to ab- initio dimer energies of a large number of dimers. After having obtained inadequate results using Hartree-Fock wavefunctions [41,63], a fit to correlated dimer energies by Matsuoka, Clementi and Yoshemine [47] resulted in the MCY model. It placed positive charges at the hydrogen sites and a negative charge on the HOH bisector — in a similar fashion to Bernal and Fowler's model. Exponential repulsions were centered at the sites of all three atoms.

Jorgensen and coworkers set out to obtain a water model that was computationally less expensive then either the ST2 or the MCY models, and at the same time provide a better description of water than these two. This study produced the TIPS family of potentials [37,38], settled with the TIP4P model [39], that is of the form of Bernal and Fowler but with different parameters. A parallel work by Berendsen and coworkers [7] resulted in the SPC potential — here the negative charge is at the oxygen site.

The list above is far from complete — they include only the models that are used most frequently. It is generally agreed upon that the main features of liquid water can be reproduced by several of them. Critical comparisons of can be found in Beveridge et al. [10], Finney, Quinn and Baum [24], Jorgensen et al. [39], Morse and Rice [56], Reimers, Watts and Klein [68].

4.2. Flexible water

The introduction of intramolecular degrees of freedom is essential for the modeling of vibrational spectra. It is also a way to introduce cooperativity into the water-water interaction through the variations in the molecular geometry, even though the atom-atom interactions are still kept pairwise additive. While at atmostpheric pressures the rigid water models appear adequate to describe the liquid structure, it is likely that for the description of water at high pressure the flexibility is necessary. They are also simpler to use in molecular dynamics simulation as the necessity of dealing with rigid-body mechanics is absent (although the calculations may become more expensive due to the necessity of smaller time step). Such models were constructed by Watts [83], Lemberg and Stillinger [45], Toukan and Rahman [81] and Bopp, Jancso and Heizinger [12].

4.3. Cooperative models

When modeling water-water interactions either the strength of the interaction or the position of the interaction centers is made dependent on the surrounding waters a cooperative model results. Campbell and Mezei [15] showed that dipole polarizability can provide an efficient way to include the effect of the surroundings. This conclusion was strengthened by the results of Clementi et al. discussed above [19], by the good agreement obtained in

subsequent calculations [16] between the calculated and experimental heats of formation of several ice forms. Furthermore, Mezei and Dannenberg recently examined the predictions of various pairwise additive models and the cooperative model of Campbell and Mezei on the low-energy trifurcated dimers [54] — a stringent test since this low energy region was not considered during the construction of any one of these potentials. For the first trifurcated structure with ab initio energy of -3.1 kcal/mol all of the pairwise additive models examined gave positive energy while the Campbell-Mezei model gave -3.7 kcal/mol. Similarly, the energy of the second trifurcated structure (ab initio value: -6.0 kcal/mol) was obtained as -5.1 kcal/mol while the best number among the pair potentials was -3.6 kcal/mol. This indicates that the inclusion of the cooperative effects in a physically meaningfull way can have the added bonus of improving the description of the dimer energy surface by producing better extrapolations for the regions of the configuration space not covered by the fitting process.

Berendsen [6] have sought to introduce cooperative effect into a water model based on point charges in a tetrahedral direction by allowing the magnitude of the charge to vary as the electric field changes. The magnitude of the change was determined in such a way that the change in the dipole moment of the molecule conformed to what the polarizability of the molecule would require. Stillinger, David and Weber have combined the Lemberg-Stillinger flexible water with an induced-dipole-related cooperative contribution [21,82]. Recently there has been a renewed interest in modeling cooperatively water interactions. Cieplak, Liebrand and Kollman [17] included an induction term into the water-water interaction model. As an alternative, Sprik and Klein [75] added terms in the time derivatives of the induced dipole vector magnitudes to the Lagrangian for use in a molecular dynamics simulation.

T a b l e 1. Quantum correction to the free energy

	ST2	MCY	TIPS	SPC	SPC	TIPS2	TIPS4	QPEN	CH
$< F^2 > *10^4$	.6236	.5718	.5242	.6608	.6524	.6675	.6793	.6238	.6583
$< N_X^2 > *10^4$	.4662	.5256	.3326	.4529	.4484	.4645	.4704	.4678	.3372
$< N_Y^2 > *10^4$	.4652	.5260	.3200	.4480	.4526	.4641	.4701	.4657	.3371
$< N_Z^2 > *10^4$	.4625	.5216	.3265	.4570	.4454	.4672	.4732	.4665	.3322
A-A_{Cl}	0.667	0.764	0.489	0.652	0.622	0.693	0.703	0.691	0.511

L e g e n d: a — $< F^2 >$ is the average square of the force acting on a molecule, in a.u.; b — $< N_i^2 >$ is the average square of the torque on the molecule around the axis i, in a.u.; c — A-A_{Cl} is the quantum correction to the free energy, in kcal/mol. d — the potentials used are as follows: ST2: Ref. 78; MCY: Ref. 47; TIPS: Ref. 37; SPC: Ref. 7; TIPS2: Ref. 38; TIP4P: Ref. 39; QPEN: Ref. 46; CH: Ref. 18.

4.4. Quantum effects

Most of the current water models are based on classical statistical mechanics, i.e. all quantum effects are mapped into the intermolecular potential. The intermolecular quantum effects, however, can still be estimated. For example, Powels and Rijkayzen [64] provide an expression for the quantum correction to the free energy of the liquid that requires

only the calculation of the force and torque-component square averages. The results of these calculations, given in Table 1, calculated from simulations using several different water models [52], show that this correction is of the order of 1 kT. Similar results were obtained by Kuharsky and Rossky [43] with the same technique and by Berens et al. by a different approach [8]. Incidentally, the magnitudes of the torque components indicate a surprisingly isotropic environment for all water models studied. The structural effect of the quantum contributions was estimated by Kuharsky and Rossky [43] and again showed a small but noticeable difference: the peak heights and through depths of the radial distribution functions decreased by 5-10% .

5. Hydrogen bonding in liquid water at standard temperature and pressure

5.1. Experimental indicators

X-ray and neutron diffraction experiments provide atom-atom radial distribution functions $g_{AB}(r)$ (i.e. the average atomic density of atom B around atom A) in water and thus are the most relevant to the hydrogen-bond structure in the liquid. They started with the pioneering work of Narten and coworkers (using mainly X-rays) [58,59,80] and were followed up by electron diffraction experiments by Palinkas et al. [61], neutron diffraction experiments by Dore and coworkers [23,29], and Soper and coworkers [73,74]. Figures 4-6 show the $g_{OO}(r)$, $g_{OH}(r)$ and $g_{HH}(r)$ obtained from the latest diffraction experiments. They support the prevalence of the linear hydrogen bond in water since (a) the most frequent O-O distance corresponds to the linear dimer O-O distance; (b) the two most frequent O-H distances correspond to the distance between the acceptor oxygen and the donor hydrogen and between the acceptor oxygen and the non-donor hydrogen in the linear dimer; (c) the average number of neighbours that is represented by the density up to the first minimum of $g_{OO}(r)$ is about four, just what would be expected from the tetrahedral picture of four hydrogen-bonded neighbours, well known from Ice Ih; (d) the position of the second peak in $g_{OO}(r)$ is at about 1.4 times the position of the first peak. This last feature is an indication that there are extensive hydrogen-bonded networks in water since it follows from the second peak's position that most hydrogen-bonded neighbours of a water have mostly hydrogen-bonded neighbours as well. In fact, reproduction of the position of the second peak in $g_{OO}(r)$ is usually taken as the first important test on a water potential.

The diffraction experiments are not the only ones that provide structural information on water. However, any other type of experiment that gives structure-related conclusions (for example, estimation of coordination numbers from the compressibility) includes further assumptions on the liquid and thus the accuracy of the numerical results depends on the (unchecked) validity of the assumptions.

5.2. Hydrogen-bond structure from computer simulations

To get further detail on the hydrogen bonds in liquid water, one has to turn to the results of computer simulation. Since the groundbreaking work of Rahman and Stillinger [65], liquid water has been simulated by a large number of potentials. Calculations with several potentials reproduced the main features of the experimental radial distributions, i.e.

the positions of the peaks and reasonable agreement was obtained with the peak heights as well, indicating that the general features of the liquid are well modeled even though the relative populations of the various possible geometries are not described too well. (It is to be mentioned, however, that the experimentally derived radial distributions also show disagreement among themselves.)

For the description of the microscopic state of a liquid Ben Naim [4] introduced the idea of quasi-component distribution function (QCDF). For a given property, the QCDF gives the mole fraction of waters for which this property has a given value. For example, the QCDF of the coordination number K, $x_c(K)$, gives the mole fraction of waters with coordination number K. Table 2 tabulates $x_c(K)$ computed from simulations using several different potentials [52,55]. The fact that $x_c(K)$ is nonzero for $0 \leq K \leq 8$ shows how far liquid water is from the Ice Ih picture, even though the average number of near neighbours is around four. Their similarity is also rather striking as the potentials in the study were developed using radically different approaches.

T a b l e 2. Comparison of the QCDF of coordination numbers for the different water models

	ST2	MCY	TIPS	SPC	TIPS2	TIP4P	QPEN	CH
$x_c(0)$	.0000	.0000	.0001	.0000	.0000	.0000	.0000	0.001
$x_c(1)$	.0000	0.001	0.004	0.002	0.001	0.001	0.001	0.013
$x_c(2)$	0.003	0.022	0.049	0.032	0.030	0.023	0.025	0.074
$x_c(3)$	0.052	0.151	0.206	0.184	0.184	0.162	0.157	0.212
$x_c(4)$	0.392	0.456	0.390	0.440	0.480	0.500	0.452	0.325
$x_c(5)$	0.341	0.290	0.260	0.266	0.245	0.251	0.273	0.246
$x_c(6)$	0.161	0.076	0.075	0.065	0.051	0.054	0.076	0.100
$x_c(7)$	0.044	0.009	0.011	0.008	0.005	0.006	0.011	0.023
$x_c(8)$	0.007	0.000	0.000	0.000	0.000	0.000	0.001	0.002
$< K >$	4.807	4.306	4.131	4.167	4.115	4.167	4.254	4.123

L e g e n d: a — The cutoff for the coordination number definition was 3.3 Å; b — the potentials as in Table 1.

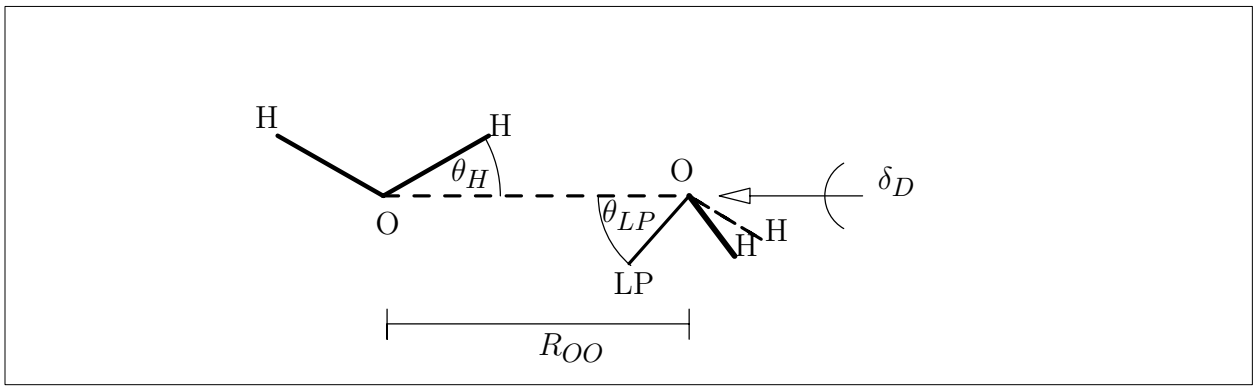

Fig. 7. Definition of the hydrogen-bond parameters R_{OO}, θ_H, θ_{LP}, δ_D.

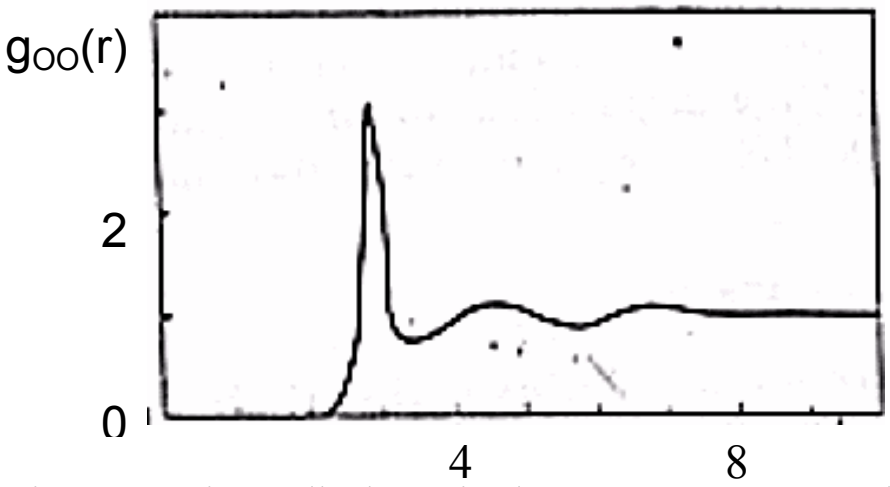

Fig. 4. Experimentally determined [74] oxygen-oxygen radial distribution function.

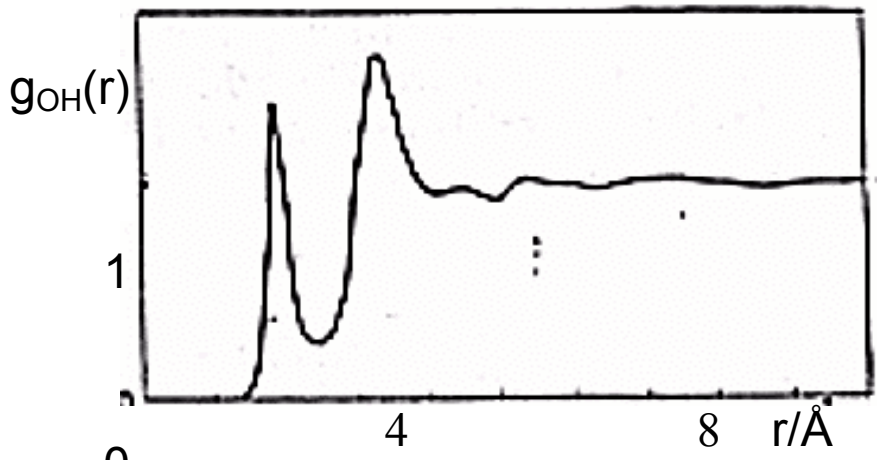

Fig. 5. Experimentally determined [74] oxygen-hydrogen radial distribution function.

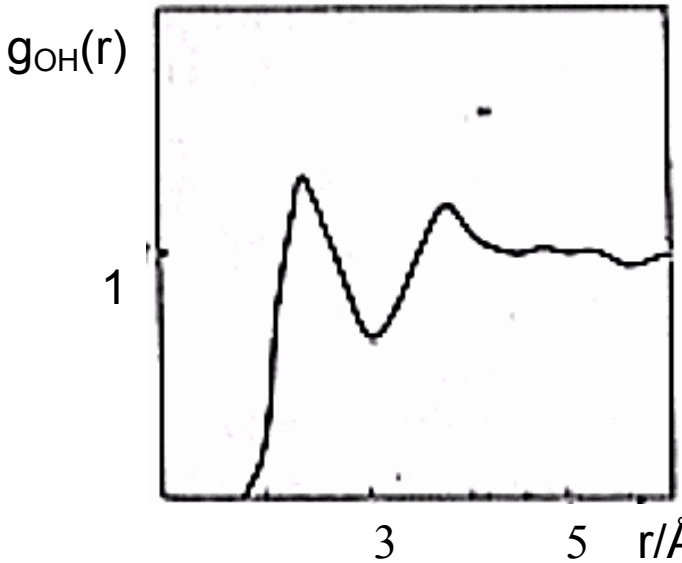

Fig. 6. Experimentally determined [74] hydrogen-hydrogen radial distribution function.

For an analysis of the hydrogen bonding one first needs an operational definition of the hydrogen bond. The geometrical parameters corresponding to an intuitive description of the hydrogen bond are defined on Figure 7, using the concept of 'lone-pair' positions (LP), a pair of points forming a tetrahedron centered on the oxygen with the two hydrogens. A hydrogen bond can be defined in terms of these parameters by requiring them to stay between certain preset limits. Alternatively, an energetic criterion can be also established. If, however, a significant number of low energy dimers different from the linear dimer occur, the energetic definition would fail to differentiate between the two.

T a b l e 3. Characterization of the strong hydrogen-bond QCDF's

	ST2	MCY	TIPS	SPC	TIPS2	TIP4P	QPEN	CH
$ROO^{\max}$	2.85	2.85	2.85	2.75	2.75	2.75	2.75	2.95
$x_H(R_{OO}^{\max})$	0.264	0.231	0.221	0.240	0.245	0.261	0.250	0.220
$\theta_H^{\max}$	12.5	17.5	12.5	12.5	12.5	12.5	12.5	17.5
$x_H(\theta_H^{\max})$	0.213	0.187	0.189	0.220	0.205	0.235	0.232	0.161
$\theta_H^{\max}$	2.5	2.5	2.5	2.5	2.5	2.5	2.5	2.5
$x_H^n(\theta_H^{\max})$	0.294	0.229	0.293	0.344	0.303	0.353	0.329	0.211
$\theta_{LP}^{\max}$	12.5	22.5	32.5	27.5	22.5	27.5	22.5	32.5
$x_H(\theta_{LP}^{\max})$	0.176	0.138	0.113	0.116	0.123	0.126	0.131	0.117
$\theta_{LP}^{\max}$	2.5	2.5	2.5	2.5	7.5	2.5	7.5	2.5
$x_H^n(\theta_{LP}^{\max})$	0.245	0.163	0.125	0.132	0.148	0.147	0.152	0.118
$\delta_D^{\max}$	5.0	5.0	5.0	5.0	25.0	5.0	5.0	5.0
$x_H(\delta_D^{\max})$	0.090	0.090	0.069	0.071	0.078	0.075	0.094	0.078

L e g e n d: a — The grid intervals are 0.1 Å, 5°, 5° and 5° for the variables R_{OO}, θ_H, θ_{LP} and δ_D, respectively; b — The variable values refer to the midpoints of the grid interval; c — Potentials as in Table 1.

Mezei and Beveridge [50] carried out a study of the distribution of these parameters on the ST2 and MCY water models, using two different geometric criteria, called the "strong" and the "weak" hydrogen bond. The strong hydrogen bond is defined by $R_{OO} < 3.0$ Å, $\theta_H \leq 45^{\circ}$, $\theta_{LP} \leq 45^{\circ}$, $\delta_D \leq 90^{\circ}$ and it was found to correspond reasonably well to a reasonable energetic cutoff, selected based on the minimum of the pair-energy frequency distribution. The weak hydrogen bond is defined by $R_{OO} \leq 4.0$ Å $\theta_H \leq 53^{\circ}$, $\theta_{LP} \leq 70.5^{\circ}$, $\delta_D \leq 180^{\circ}$. Figures 8-11 show the QCDF's of the four hydrogen-bond parameters for the MCY water. They again confirm the intuitive picture of the hydrogen bond. An interesting feature of the QCDF's of the angles H and LP is that their peak is not at 0°, i.e. most of the hydrogen bonds are bent. While at first it appears to be a contradiction with the linear hydrogen bond assumption, it can be understood as a statistical effect: the configuration space volume of hydrogen bonds with angles θ_H and θ_{LP} are proportional to sin θ_H and sin θ_{LP}, respectively. As Figures 9 and 10 also show, when this volume contribution is factored out, the preference toward linear hydrogen bonds become evident. Later studies of other water models showed similar picture. In Table 3 the main features of the calculated hydrogen-bond distributions from several different simulations are compared for the strong hydrogen bond [50,55]. Belch, Rice and Sceats [3] used a combination of H, LP and the H-LP

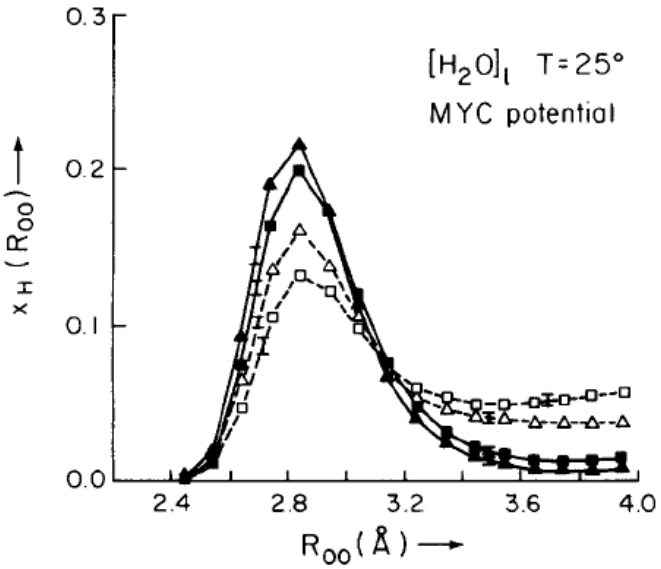

Fig. 8. QCDF's for the hydrogen-bond parameter R_{OO}. MCY water at 25°C [50].
■: $x_H(R_{OO})$, strong hydrogen bond,
▲: $x_H(R_{OO})/(4\pi R^2_{OO})$, strong hydrogen bond,
□ : $x_H(R_{OO})$, weak hydrogen bond,
Δ : $x_H(R_{OO})/(4\pi R^2_{OO})$, weak hydrogen bond.

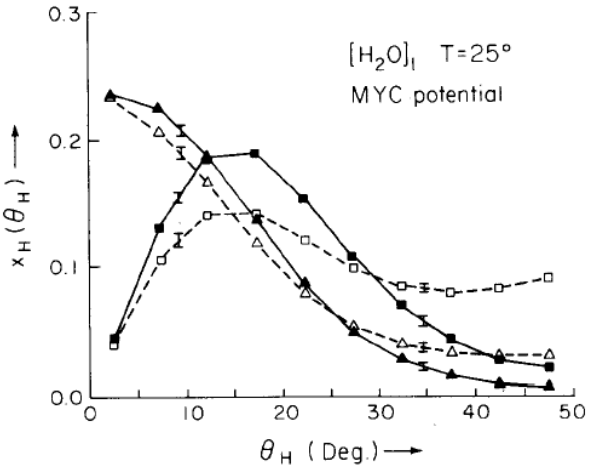

Fig. 9. QCDF's for the hydrogen-bond parameter θ_H. MCY water at 25°C [50]. Symbols as in Figure 8.

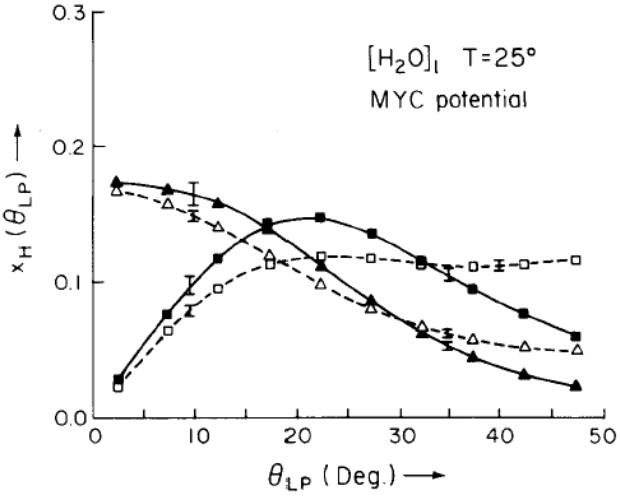

Fig. 10. QCDF's for the hydrogen-bond parameter θ_{LP}. MCY water at 25°C [50]. Symbols as in Figure 8.

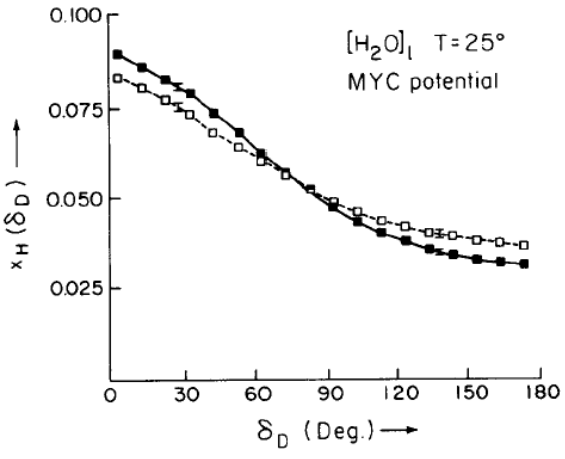

Fig. 11. QCDF's for the hydrogen-bond parameter δ_D. MCY water at 25°C [50]. Symbols as in Figure 8.

distance as a geometric criterion and found that for the ST2 water a close correspondance exist between their geometric and the energetic hydrogen bond definition, although some waters close to the energy treshold may not be geometrically hydrogen bonded.

5.3. Hydrogen-bonded networks

As discussed earlier, the possibility of two acceptor and two donor hydrogen bonds gives rise to an easy development of hydrogen-bonded networks. Geiger, Stillinger and Rahman [28] analyzed computer simulation histories of the ST2 model (at different temperatures) from this point of view. They used an energetic criterion of hydrogen bond and found that the average number of hydrogen bonds per water nHB is a monotonous (actually, nearly linear) function of the energy cutoff. Treating the formation of the hydrogen-bonded networks as a percolation phenomenon, the found that, in good agreement with Stockmayer's theory [79], the percolation threshold of liquid water is $n_{HB} >\sim 1.3$. This means that, for most reasonable hydrogen-bond definitions, water can be considered a hydrogen-bonded gel.

Mezei and Beveridge extended their studies using the geometric hydrogen-bond criterion on simulation histories of the ST2 and MCY models (also at different temperatures). When the number of waters with no hydrogen bonds was plotted against nHB, the resulting curve was found invariant to the potential or to the choice of hydrogen-bond criterion. This fit very well into the percolation model of liquid water proposed by Stanley [76]. The percolation model assumed that at most 4 hydrogen bonds can be formed per water, and individual bonds form with probability $p_{HB} = n_{HB}/4$. The first prediction of this model gives the distribution of clusters with N waters as a function of pHB as a simple binomial expression (for $N = 1$ this is exactly the number of unbonded water studied earlier). The formula also performed well for $N > 1$ when compared with computer simulation results, especially for $n_{HB} < 2.5$. An additional, more subtle consequence of the model (following only from combinatorial arguments) is the clustering of 4-bonded waters. This is rather remarkable, since the idea of water consisting of a mixture of 4-bonded, ice-like "structured" water and more disordered water has been discussed since Roentgen [69]. In analogy with the comparison of the density of Ice Ih and water, these 4-bonded regions should have lower density than the other regions of the liquid. Computer simulation results were analyzed by Geiger and Stanley [27], Rapaport [66] and Mezei [49]. In most cases, small density deviations were obtained but, depending on the volumes considered in the density calculations, the results were contradictory. For the ST2 water, using the energetic hydrogen bond definition, however, the density around the 4-bonded waters was found to decrease unequivocally. Experimental evidence is based on small- angle X-ray scattering experiments [14]: the structure factor $S(q)$ shows an anomalous increase with decreasing q that is interpreted as evidence for enhanced density fluctuations. As predicted, the effect becomes more pronounced as the water is supercooled and becomes negligible with the introduction of impurities.

Care should, however, be exercised when this idea of "two kinds of waters" is made into a quantitative model. While it is tempting to simply assume real water as a mixture of these two different kinds of waters and assign particular properties to each type, resulting in a quantitative model for the properties of liquid water (as it has indeed been done), Kauzmann has shown that such model is internally inconsistent [40]. Specifically, he showed that if water is assumed to consist of structured clusters of N water molecules in a "sea" of unstructured waters then the experimental data for the temperature dependence of the thermal expansion coefficient requires $N \simeq 40$ while the experimental temperature dependence of the heat

capacity can only be reproduced with N near unity. Thus this concept of the two kinds of waters must be included in a more complex way — possibly with a continuum of water types.

5.4. Hydrogen-bond lifetime

If most neighbours of a water can be assumed to be hydrogen bonded the time required for a molecule to diffuse away from its neigbour indicates the time during which a hydrogen bond is intact. Hertz estimated the residence time as the time required for a water molecule to diffuse from the first peak of $g_{OO}(r)$ to the second peak, 8 ps [33]. Impey, Madden and McDonald [36] found that the correlation time for the persistence of waters in the first shell of a water is 1.8 ps in the MCY water. As this quantity gives roughly the time required for a water molecule to diffuse from the first peak of $g_{OO}(r)$ to the first minimum, there is reasonable correspondence with Hertz's estimate. However, for most "reasonable" definition of hydrogen bonds there are almost always neighbours that are not hydrogen bonded therefore the numbers above are to be considered a lower bound for the hydrogen-bond lifetime.

Rapaport followed the breaking and forming of hydrogen bonds [67] (energetic criterion) in his simulation of the MCY water. Waters displayed an oscillatory behaviour - hydrogen bonds broke with an exponential time-constant of 0.05-0.3 ps but in most cases the bond was reformed. The time constant of the "irrevocable" breaking of hydrogen bonds was found to be larger, in the 1-10 ps range. This is basically in accord with the experimentally observed characteristic times for intermolecular vibration and diffusion, 0.07 ps and 18 ps, respectively: a hydrogen bond breaks after cca 20-100 vibrations.

Sciortino and Fornili [71] examined a 20 ps molecular dynamics run of ST2 water. They proposed a combined energetic, geometric and temporal definition of hydrogen bond: a pair is considered hydrogen bonded that stays within 3.5 Å with attractive energy for at least 0.4 ps. It was found that hydrogen-bonds that persist longer have larger peaks in their hydrogen-bond angle QCDF's and a larger abundance of waters with four hydrogen-bonded neighbours, indicating the prevalence of better developed bonds among the longer lived ones. The time constant of a hydrogen bond was found to be 2.0 ps — in the same range as the studies discussed above.

5.5. Energetic considerations

The hydrogen-bond QCDF's discussed earlier indicate that in the liquid state the deviation from the linear hydrogen bond is the "norm" and the occurrence of water pairs with minimum energy is a rare event. This conclusion can be quantified by the calculation of the QCDF of the pair-energy $x_P(\epsilon)$, defined as the mole fraction of neighbours within 3.3 Ao with energy . For all water models examined, $x_P(\epsilon)$ was found to have a single peak, drop sharply to zero at the minimum of the water water potential and approach zero much slower in the positive direction, indicating the existence of some repulsive pairs [52,55]. Table 4 gives the characteristics of $x_P(\epsilon)$ calculated for several water models.

The average-near neighbour pair energy, in conjunction with the average number of hydrogen bonds can give an indication of the share of hydrogen bonds in the total energy of the liquid. For example, the average pair energy of the MCY water is 3.0 kcal/mol. Using the "strong" geometric definition of a hydrogen bond, n_{HB} was found to be 2.1 , resulting in an

average total hydrogen bond energy of 6.2 kcal/mol. As the average total binding energy of a water molecule in the MCY water is 17.4 kcal/mol [55], this suggests a cca 30% contribution from hydrogen bonds to the total energy. Even if all first-shell neighbours are considered to be hydrogen bonded, there is about 30% of the energy that comes from interactions with waters outside the first shell since for the MCY water $\langle K \rangle = 4.3$. Similar conclusions hold for the other water models.

T a b l e 4. Characterization of the QCDF $x_P(\epsilon)$

	ST2	MCY	TIPS	SPC	TIPS2	TIP4P	QPEN	CH
$\epsilon^{\max}$	-4.60	-4.40	-4.10	-5.10	-4.80	-4.70	-5.00	-4.30
$x_P(\epsilon^{\max})$	0.0531	0.0581	0.0522	0.0514	0.0306	0.0309	0.0581	0.0316
$\epsilon_<^{99.9}$	-6.60	-5.60	-5.60	-6.50	-6.10	-6.10	-6.40	-5.50
$\epsilon_>^{99.9}$	5.40	5.20	>2.90	>2.90	>2.90	>2.90	4.40	>2.90
$\epsilon_<^{1/2}$	-5.60	-5.20	-5.20	-6.10	-5.70	-5.70	-5.80	-5.10
$\epsilon_>^{1/2}$	-2.60	-2.20	-1.80	-2.80	-2.80	-3.00	-3.00	-2.30

Legend: a — The grid sizes were 0.2 kcal/mol; b — max is the right end point of the grid where the maximum of $x_P(\epsilon)$ is; c — the value of the maximum is $x_P(\epsilon^{\max})$; d — $\epsilon_<^{99.9}$ and $\epsilon_>^{99.9}$ give the beginning and end point of the smallest interval that contains 99.9% of the distribution; e — $\epsilon_{<1/2}^{99.9}$ and $\epsilon_{>1/2}^{99.9}$ give the smallest and largest values such that $x_P(\epsilon) = x_P(\epsilon^{\max})/2$; f — Potentials as in Table 1.

6. Hydrogen bonding in liquid water under non-standard conditions

Both experimental and theoretical studies were performed on water at high and low temperatures and pressures. The common result of these studies was the remarkable persistence of the hydrogen bond.

6.1. Diffraction results

Narten and Levy extended their X-ray diffraction measurements up to 200°C [59]. The position of the first peaks in the atom-atom distributions remained virtually unchanged, but the peak heights were lowered - an indication of the persistence of the hydrogen bonds but also an increased disorder. The second peak of $g_{OO}(r)$, on the other hand, moved out to about twice the first peak's distance. This indicates the appearance of a significant number of non-tetrahedral neighbours. Neutron diffraction studies of Gibson and Dore [29] in the 11°C-75°C range showed a slight increase in the O-D distance with the increase in temperature. Neutron diffraction experiments in the supercooled region by Bosio et al. [13] showed the same trend and also gave indication of enhanced orientational structre.

Gabella and Neilson performed X-ray diffraction measurements on light and heavy water up to 6 kbar pressure(i.e. at 1.152 g/cm^3) [26]. Simply scaling the down the distances by 5% would produce the density at 6 kbar. The O-O and the O-H distances at 6 kbar were found to be shortened by less than half of this scaled amount: 0.05 Å and 0.03 Å, respectively. This can be considered an indication of the resistance of a hydrogen bond to pressure.

6.2. Computer simulation studies

Mezei and Beveridge simulated the MCY water at 25^{o}C, 37^{o} and 50o at the respective experimental densities [51]. No shift in the peak position was observed but the peak hights decreased slightly with the increase in temperature. Impey, Klein and McDonald studied the MCY water at high density (i.e. under high pressure) and at high temperatures [35]. The high temperature results were in qualitative agreement with the X-ray results of Narten, Danford and Levy [58]. The high-density study was run at 1.345 g/cm^3 (corresponding to 22 kbar pressure). The first peak position of $g_{OO}(r)$ is shortened by only 0.04 Å, an order of magnitude smaller than simple scaling would cause. Similar behaviour was observed for $g_{OH}(r)$ and $g_{HH}(r)$.

Palinkas et al. examined the hydrogen-bond structure of their modified central-force model [12] also at 1.345 g/cm^3 density [60]. The mean O-O distance is decreased only by 0.1 Å. This is larger than the change for the MCY but is less than a third of what the density scaling would indicate — again confirming the strong integrity of hydrogen bond under pressure. The density increase is instead achieved by an increase in the deviation from tetrahedrality. The stronger distortions can then provide room for additional waters in the first shell. As a consequence, significant distortion of the hydrogen-bond angles was found and the average number of hydrogen bonds decreased from 1.9 to 1.3 .

Mountain studied the TIP4P water at lower densities (i.e. expanded water) and at elevated temperatures [57]. Increasing only the temperature showed similar behaviour as described earlier: lowering peak heights and moving the second peak farther out. The first peak of $g_{OH}(r)$, called by Mountain the "hydrogen- bond peak", gets progressively smaller as the temperature is increased and disappears at cca 780 K temperature for all pressures studied. Using a simple geometric criterion for the hydrogen bond (O-H distance less than 2.4 Ao), hydrogen bonds were found to persist even at supercritical temperatures. He also found that for densities above 0.45 g/cm^3 the average hydrogen bond scaled by the number density, $n_{HB}/(N/V)$, is a simple (nearly linear) decreasing function of the temperature, but the scaling does not hold for lower densities.

7. Summary

We have seen that the water-water interaction energy surface is a rather complex one allowing different types of hydrogen bonds. Out of these the linear hydrogen bond dominates the liquid water structure. Several unusual properties of the linear hydrogen bond contribute to the anomalous properties of liquid water: a) it is rather strong therefore persists for several picoseconds in a wide temperature and pressure range; b) it is strongly orientation dependent, resulting in unusual density patterns; c) the balance between the acceptor and donor hydrogen bonds allow the formation of extended networks; d) the tetrahedral directionality yields a large number of energetically (nearly) equivalent configurations with different orientations for a given arrangement of molecular centers thereby reducing the entropic penalty for the orientational restrictions; e) the geometry of the hydrogen-bonded networks does not work against the contribution of distant neighbours through electrostatic interactions.

8. Acknowledgements

This work was supported under an RCMI grant #SRC5G12RR0307 from NIH to Hunter College, under a CUNY/PSC grant, as well as under NIH grant GM-24914 and NSF grant CHE-8203501 to Prof. D.L. Beveridge. Computing resources were provided by the City University of New York, University Computing Center. While the formation of the picture of liquid water presented here was helped by discussions with many collegues, collaboration with Profs. D.L. Beveridge and E.S. Campbell had by far the most important impact for which the author wishes to express his gratitude.

1. *P. Barnes, J.L. Finney, J.D. Nicholas and J.E. Quinn.,* Nature, **282,** 459 (1979).

2. *P.O. Baum and J.L. Finney,* Mol. Phys., **55,** 1097 (1985).

3. *A.C. Belch, S.A. Rice and M.G. Sceats,* Chem. Phys. Letters, **77,** 455 (1981).

4. *A. Ben-Naim,* "Water and Aqueous Solutions", Plenum Press, New York (1974).

5. *A. Ben-Naim and F.H. Stillinger,* in "Structure and Transport Processes in Water and Aqueous Solution", R.A. Horne, Ed., Wiley, New York (1972).

6. *H.J.C. Berendsen,* in "Molecular Dynamics and Monte Carlo Calculations on Water", Report CECAM Workshop, Orsay, France, p63 (1972).

7. *H.J.C. Berendsen, J.P.M. Postma, W.F. van Gunsteren and J. Hermans,* in "Jerusalem Symposia on Quantum Chemistry and Biochemistry", 1981, B. Pullman, editor, Reidel Publ. Dordrecht, Holland.

8. *P.H. Berens, D.H. Mackay, G.M. White and K.R. Wilson, J.* Chem. Phys., **79,** 2375 (1983).

9. *J.D. Bernal and R.H. Fowler,* J. Chem. Phys., **1,** 515 (1933).

10. *D.L. Beveridge, M. Mezei, P.K. Mehrotra, F.T. Marchese, G. Ravishanker, T.R. Vasu and S. Swaminathan,* in "Molecular based study and perdiction of fluid properties", J.M. Haile and G. Mansoori, eds., Advances in Chemistry Series, Vol 204, American Chemical Society, (1983).

11. *R.L. Bloomberg, H.E. Stanley, A. Geiger and P. Mausbach, J.* Chem. Phys., **80,** 5230 (1984).

12. *P. Bopp, H. Jancso and K. Heizinger,* Chem. Phys. Lett., **98,** 129 (1983).

13. *L. Bosio, J. Texeira, J.C. Dore, D.C. Steytler and P. Chieux,* Mol. Phys., **50,** 733 (1983)

14. *L. Bosio, J. Texeira and H.E. Stanley,* Phys. Rev. Letters, **46,** 547 (1981).

15. *E.S. Campbell and M. Mezei,* J. Chem. Phys., **67,** 2338 (1977).

16. *E.S. Campbell and M. Mezei,* Mol. Phys., **41,** 883 (1980).

17. *P. Cieplak, T.P. Lybrand and P.A. Kollman,* J. Chem. Phys., **86,** 6393 (1987).

18. *E. Clementi and P. Habitz,* J. Phys. Chem., **87,** 2815 (1983).

19. *E. Clementi, W. Kolos, G.C. Lie and G. Ranghino,* Int. J. Quant. Chem., **17,** 377 (1980).

20. *J.J. Dannenberg,* J. Phys. Chem., **92,** 6869 (1988).

21. *C.W. David and F.H. Stillinger,* J. Chem. Phys., **69,** 1473 (1978).

22. *M.J.S. Dewar, E.G. Zoebisch, E.G. Healy and J.J.P. Stewart,* J. Am. Chem. Soc., **107,** 3902 (1985).

23. *J.C. Dore,* Farad. Disc., **66,** 82 (1978).

24. *D. Eisenberg and W. Kauzmann,* "The Structure and Properties of Water", Oxford Univ. Press, New York (1969).

25. *J.L. Finney, J.E. Quinn and J.O. Baum,* in "Water Science Reviews", Vol. 1, F. Franks, ed., Cambridge Univ. Press (1985).

26. *G.A. Gaballa and G.W. Neilson,* Mol. Phys., **50,** 97 (1983).

27. *A. Geiger and H.E. Stanley,* Phys. Rev. Letters, 49, 1749 (1982).

28. *A. Geiger, F.H. Stillinger, and A. Rahman,* J. Chem. Phys., **70,** 4185 (1979).

29. *I.P. Gibson and J.C. Dore,* Mol. Phys., **48,** 1019 (1983).

30. *D. Hankins, J.W. Moskowitz and F.H. Stillinger,* J. Chem. Phys., **53,** 4544 (1970).

31. *P.C. Hariharan and J.A. Pople,* Mol. Phys., **27,** 209 (1974).

32. *W.J. Hehre, R. Ditchfield and J.A. Pople,* J. Chem. Phys., **56,** 2257 (1972).

33. *H.G. Hertz,* in "Water: A Comprehensive Treatise", Vol. 3, F. Franks, ed., Plenum Press, New York (1983).

34. *F. Hirata and P.J. Rossky,* Chem. Phys. Letters, **83,** 329 (1981).

35. *R.W. Impey, M.L. Klein, and I.R. McDonald,* J. Chem. Phys., **74,** 647 (1981).

36. *R.W. Impey, P.A. Madden and I.R. McDonald,* J. Phys. Chem., **87,** 5071 (1983).

37. *W.L. Jorgensen,* J. Am. Chem. Soc., **103,** 335 (1981).

38. *W.L. Jorgensen,* J. Chem. Phys., **77,** 4156 (1982).

39. *W.L. Jorgensen, J. Chandrasekhar, J.D. Madura, R.W. Impey and M.L. Klein,* J. Chem. Phys., **79,** 926 (1983).

40. *W. Kauzmann,* Colloques Internationaux du C.N.R.S. **#246,** 63 (1976).

41. *H. Kistenmacher, H. Popkie, E. Clementi, and R.O. Watts, J.* Chem. Phys., **60,** 4455 (1974).

42. *A.I. Kitaigorodsky, K.V. Mirskaya and V.V. Nauchatel,* Kristallogaphija, **14,** 900 (1969).

43. *R.A. Kuharshy and P.J. Rossky,* J. Chem. Phys., **82,** 5164 (1985).

44. *L. Lang and H.D. Ludemann,* Angew. Chem. Int. Ed. Engl., **21,** 315 (1982).

45. *H.L. Lemberg, F.H. Stillinger,* J. Chem. Phys., **62,** 1677 (1975).

46. *F.T. Marchese, P.K. Mehrotra and D. L. Beveridge,* J. Phys. Chem., **85,** 1 (1881).

47. *O. Matsuoka, E. Clementi and M. Yoshimine,* J. Chem. Phys., **64,** 1351 (1976).

48. *N. Metropolis, A.W. Rosenbluth, M.N. Rosenbluth, A.H. Teller, and E. Teller,* J. Chem. Phys., **21,** 1087 (1953).

49. *M. Mezei,* Mol. Phys., **52,** 1003 (1984).

50. *M. Mezei and D.L. Beveridge,* J. Chem. Phys., **74,** 622 (1981).

51. *M. Mezei and D.L. Beveridge,* J. Chem. Phys., **76,** 593 (1982).

52. *M. Mezei and D.L. Beveridge,* unpublished results.

53. *M. Mezei and E.S. Campbell,* unpublished results.

54. *M. Mezei and J.J. Dannenberg,* J. Phys. Chem., **92,** 5860 (1988).

55. *M. Mezei, S. Swaminathan and D.L. Beveridge,* J. Chem. Phys., **71,** 3366 (1979).

56. *M.D. Morse and S.A. Rice,* J. Chem. Phys., **76,** 650 (1982).
57. *R.D. Mountain,* J. Chem. Phys., **90,** 1866 (1989).
58. *A.H. Narten, M.D. Danford, and H.A. Levy,* Disc. Faraday Soc., **43,** 97 (1967).
59. *A.H. Narten and H.A. Levy,* J. Chem. Phys., **55,** 2263 (1971).
60. *G. Palinkas, P. Bopp, G. Jancso and K. Heizinger,* Z. Naturforsch., **39a,** 179 (1984).
61. *G. Palinkas, E. Kalman and P. Kovacs,* Mol. Phys., **34,** 525 (1977).
62. *B.M. Pettitt and P.J. Rossky,* J. Chem. Phys., **77,** 1451 (1982)
63. *H. Popkie, H. Kistenmacher and E. Clementi,* J. Chem. Phys., **59,** 1235 (1973).
64. *J.G. Powles and G. Rickayzen,* Mol. Phys., **38,** 1875 (1979).
65. *A. Rahman and F.H. Stillinger,* J. Chem. Phys., **55,** 336 (1971).
66. *D.C. Rapaport,* Molec. Phys., **48,** 23 (1983).
67. *D.C. Rapaport,* Molec. Phys., **50,** 1151 (1983).
68. *J.R. Reimers, R.O. Watts and M.L. Klein,* Chem. Phys., **64,** 95 (1982).
69. *W. Roentgen,* Ann. Phys., **45,** 91 (1892).
70. *G.N. Sarkisov, Dashevsky, and G.G. Malenkov,* Mol. Phys., **27,** 1249 (1974).
71. *F. Sciortino and S.L. Fornili,* J. Chem. Phys., **90,** 2786 (1989).
72. *J. Snir, R.A. Nemenoff and H.A. Scheraga,* J. Phys. Chem., **82,** 2497 (1978).
73. *A.K. Soper and R.N. Silver,* Phys. Rev. Lett., **49,** 471 (1982).
74. *A.K. Soper and M.G. Philips,* Chem.Phys., **107,** 47 (1986).
75. *M. Sprik and M.L. Klein,* J. Chem. Phys., **89,** 7556 (1988).
76. *H.E. Stanley, J.* Phys. A, L211 (1979).
77. *H.E. Stanley and J. Teixeira,* J. Chem. Phys., **73,** 3404
(1980).
78. *F.H. Stillinger and A. Rahman,* J. Chem. Phys., **60,** 1545 (1974).
79. *W.H. Stockmayer,* J. Chem. Phys., **11,** 45 (1943).
80. *W.E. Thiessen, L. Blum and A.H. Narten, Science,* **217,** *1033 (1982).*
81. K. Toukan and A. Rahman, Phys. Rev., B31, 2643 (1985).
82. *T.A. Weber and F.H. Stillinger,* J. Chem. Phys., **77,** 4150 (1982).
83. *R.O. Watts, Chem. Phys.,* **26,** 367 (1977).

Department of Chemistry and Center for Study
in Gene Structure and Function,
Hunter College and the Graduate Center
of the CUNY, New York, NY 10021, USA.

Received 12.09.89